# Characterization of $C_2S_4^{\cdot+}$ isomers by mass spectrometry and ab initio molecular orbital calculations

Pascal Gerbaux[a,†], Robert Flammang[a,*], Curt Wentrup[b], Ming Wah Wong[c]

[a]*Organic Chemistry Laboratory, University of Mons-Hainaut, Avenue Maistriau 19, B-7000 Mons, Belgium* [b]*Department of Chemistry, The University of Queensland, Brisbane 4072 Qld., Australia* [c]*Department of Chemistry, The National University of Singapore, Kent Ridge, 119260 Singapore*

## Abstract

Isomeric $C_2S_4^{\cdot+}$ radical cations, a dimer $(CS_2)CS_2^{\cdot+}$ and a covalently bounded $C_2S_4^{\cdot+}$ species, are generated by chemical ionization (self-chemical ionization conditions) of carbon disulfide or by dissociative electron ionization of 1,3,4,6-tetrathiapentalene-2,5-dione and 1,2-dithiolo[4,3-c][1,2]dithiole-3,6-dione, respectively. These ions are structurally characterized making use of mass spectrometric methodologies such as collisional activation, neutralization–reionization and ion–molecule reactions performed in a hybrid tandem mass spectrometer of sector–quadrupole–sector configuration. These experimental results are supported by ab initio calculations of the relative energies of 19 possible isomers indicating that the most stable $C_2S_4^{\cdot+}$ structure corresponds to a $CS_2$ dimer with a $C_2$ symmetry, 52 kJ mol$^{-1}$ more stable than the lowest-energy covalently bound structure consisting of a four-membered ring thioketene species. (Int J Mass Spectrom 210/211 (2001) 31–42) © 2001 Elsevier Science B.V.

## 1. Introduction

The chemical ionization of carbon disulfide (self-chemical ionization conditions) leads, beside the molecular ions $CS_2^{\cdot+}$ and the fragments resulting from unimolecular dissociations, to the generation of a series of $C_xS_y^{\cdot+}$ ions [1]: $C_2S_n^{\cdot+}$ ($n = 2$–4) and $CS_n^{\cdot+}$ ($n = 3$–4). With the notable exception of $CS_3^{\cdot+}$ ions (5% relative to the *m/z* 76 base peak) and

$C_2S_2^{\cdot+}$ ions (1%), all the other species are by far less abundant ($<<$1%).

Several mass spectrometric studies were performed in order to elucidate the actual structure of some of these $C_xS_y^{\cdot+}$ ions. For instance, ethene dithione radical cation, $S=C=C=S^{\cdot+}$, is presently a well-defined species easily generated by dissociative ionization of various heterocyclic precursors [2]. The atom connectivity of this ion was clearly established by collisional activation (CA) and the intrinsic stability of the corresponding neutral molecule was unambiguously confirmed by neutralization–reionization (NR) and NR/CA experiments.

The most abundant ion–molecule reaction product observed in the chemical ionization source is the *m/z*

108 radical cation, $CS_3^{.+}$. The CA spectrum of these ions suggests [3] the carbon disulfide $S$-sulfide connectivity, SCSS, but a similar pattern is also expected for the isomeric carbon disulfide $C$-sulfide connectivity, SC(S)S. In fact, nearly identical CA spectra of the $CS_3^{.+}$ ions were obtained upon dissociative ionization of the isomeric dithioledithiones **1** and **2** [4]. That may be indicative of the occurrence of a mixture of isomers or that the SC(S)S$^{.+}$ isomer rearranges into the more stable SCSS$^{.+}$ radical cation; SCSS$^{.+}$ was calculated more stable than SC(S)S$^{.+}$ by 42.4 kJ/mol at the G2(MP2,SVP) level of theory [3]. Ion–molecule reactions of the $CS_3^{.+}$ radical cations with acetonitrile were shown to produce $CH_3CNS^{.+}$ and $CH_3CNSS^{.+}$ ions and the occurrence of the SS$^{.+}$ transfer reaction has been interpreted in terms of the presence of the more stable isomer, SCSS$^{.+}$ [3].

Dissociative ionization of 1,3,4,6-tetrathiapentalene-2,5-dione [3] and 1,2-dithiolo[4,3-c][1,2]dithiole-3,6-dione [4] were used for the production of $C_2S_3^{.+}$ radical cations [5]. Collisional activation (high or low translational energy regime) and neutralization–reionization mass spectrometries were found inefficient for the unambiguous identification of the connectivity of these ions. In contrast, ion–molecule reactions (in particular with nitric oxide) allowed a clear differentiation of the $C$-sulfide ethene dithione ion, $SCCS_2^{.+}$, and the $S$-sulfide ethene dithione ion, $SCCSS^{.+}$ [5]. These results indicated that the $C_2S_3^{.+}$ radical cations generated by chemical ionization of carbon disulfide possess the $C$-sulfide ethene dithione connectivity, $SCCS_2^{.+}$ [6], in agreement with the fact that $SCCS_2^{.+}$ was calculated to be the more stable isomer by 91.3 kJ mol$^{-1}$ [5]. Gas phase protonation of ethene dithione also occurs on a carbon atom, not on sulfur [7].

This article reports on the structure and reactivity of the $C_2S_4^{.+}$ radical cations produced in a high pressure ion source making use of tandem mass spectrometric methodologies in a hybrid mass spectrometer of sector-quadrupole-sector configuration. Ions of $C_2S_4$ composition are also generated from heterocyclic precursors **3** and **4** (Scheme 1), which lose consecutively two carbon monoxide molecules after electron ionization. In addition, ab initio calcu-
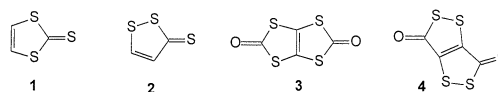


Scheme 1.

lations are employed to determine the structures and energies of isomeric $C_2S_4^{.+}$ radical cations.

## 2. Experimental

The spectra were recorded on a large scale tandem mass spectrometer (Micromass AutoSpec 6F, Manchester) combining six sectors of $c_1E_1B_1c_2E_2c_3c_4E_3B_2c_5E_4$ geometry (E stands for electric sector, B for magnetic sector, and c for collision cell) [8]. General conditions were 8 kV accelerating voltage, 200 $\mu$A trap current (in the electron ionization mode, EI), 1 mA (in the chemical ionization mode, CI), 70 eV ionizing electron energy and 200 °C ion source temperature. The samples were introduced with a direct insertion probe or via a heated (180 °C) septum inlet.

Collisional activation ($O_2$) of fast (8 keV kinetic energy) mass selected ions was performed in $c_4$ and the CA spectra [Fig. 1(a) and (c)] were recorded by scanning the field of $E_3$ and collecting the ions in the fifth field-free region with an off-axis photomultiplier detector. The NR (Xe/$O_2$) unit was situated in the fourth field-free region, $c_3$ and $c_4$ being the neutralization and the reionization cells, respectively. The NR spectra [Fig. 1(b) and (d)] were recorded in a similar way, the collisional reionization with oxygen in $c_4$ being preceded by collisional reduction of the ions with xenon in $c_3$.

The installation of an rf-only quadrupole collision cell (Qcell) inside the instrument between $E_2$ and $E_3$ was also reported elsewhere [9]. This modification allows the study of associative ion–molecule reactions and the study of collisional activation of decelerated ions. Briefly, the experiments utilizing the Qcell consist of the selection of a beam of fast ions (8 keV) with the three first sectors ($E_1B_1E_2$), the deceleration of these ions to approximately 5 eV (to maximize ion–molecule reactions) or 20–30 eV (to maximize collision-
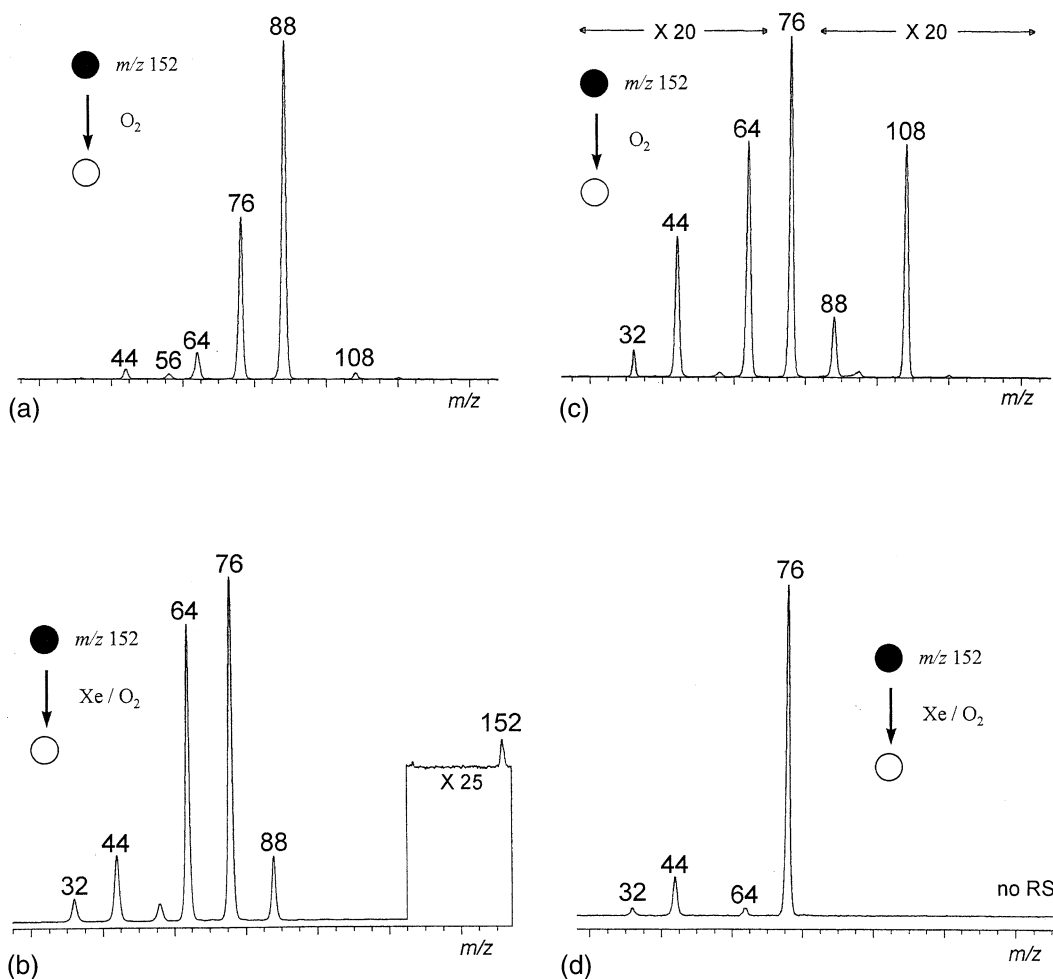
Fig. 1. CA ($O_2$) mass spectrum of the $C_2S_4^{\cdot+}$ ions (*m/z* 152) generated by dissociative ionization of the tetrathiapentalene **3** (the same spectrum is obtained starting with **4**) (a) and NR (Xe/$O_2$) of the same ions (b). CA (c) and NR (d) of the $C_2S_4^{\cdot+}$ ions generated by self-chemical ionization of carbon disulfide. The terminology used to schematize the ion–molecule reactions is that introduced by Schwartz et al.: a filled circle represents a fixed (or selected) mass; an open circle, a variable (or scanned) mass, whereas the neutral reagent or collision gas that causes the mass transitions is shown between the circles [22].

induced dissociations). The interaction between the ions and the reagent gas (the pressure of the gas is estimated to be about $10^{-3}$ Torr) is thereafter realized in the Qcell and, after reacceleration at 8 keV, all the ions generated in the quadrupole are separated and mass-measured by scanning the field of the second magnet. The high energy CA spectra of mass-selected ions generated in the Qcell can be recorded by a linked scanning of the fields of the last three sectors.

All the samples were commercially available (Al-drich, Resco Trade) and used without further purification, except for 1,2-dithiolo[4,3-c][1,2]dithiole-3,6-dione [**4**] which is prepared according to a procedure described in the literature [10].

## 3. Mass spectrometric results

### 3.1. Production of $C_2S_4^{\cdot+}$ (m/z 152) radical cations

As previously described [1,3], CI of carbon disul-fide produces inter alia $C_2S_4^{\cdot+}$ ions (*m/z* 152) radical

cations. These ions can also be prepared in the quadrupolar collision cell of our mass spectrometer by interaction between decelerated $CS_2^{\cdot+}$ molecular ions and neutral $CS_2$ [3]. $C_2S_4^{\cdot+}$ ions were also generated by photoionization [11] or electron ionization [12] of the neutral van der Waals dimer. In these experiments, the neutral carbon disulfide dimer was produced in an adiabatic gas expansion of a mixture of $CS_2$ vapour and argon [11,12].

After electron ionization, the molecular ions $\mathbf{3}^{\cdot+}$ consecutively eliminate two molecules of carbon monoxide, the relative intensity of the corresponding signal ($m/z$ 152) in the mass spectrum amounts 25%. Based on the structure of the neutral precursor, the intermediate radical cation ($m/z$ 180) is likely to possess the structure $\mathbf{a}$ presented in Scheme 2.

The electron ionization of the isomeric molecule $\mathbf{4}$ also induces the losses of two molecules of carbon monoxide, but this two-step process is much less efficient than the corresponding dissociation starting from $\mathbf{3}^{\cdot+}$. Actually, the $m/z$ 152 signal in the mass spectrum represents only 2% of the intensity of the base peak ($m/z$ 208). The structure of the intermediate radical cation ($\mathbf{b}$ in Scheme 2) should be different from $\mathbf{a}$ on the basis of the structure of the neutral precursor molecules $\mathbf{4}$. Indeed, the CA spectra of these species (not shown) are completely different: for instance, the CA spectrum of ions $\mathbf{b}$ features intense peaks at $m/z$ 116 (loss of $S_2$), $m/z$ 96 ($S_3^{\cdot+}$), and $m/z$ 84 ($C_3OS^{\cdot+}$) (not observed for ions $\mathbf{a}$). The reaction sequence $\mathbf{4}^{\cdot+} \rightarrow \mathbf{4}^{\cdot+} - CO \rightarrow \mathbf{4}^{\cdot+} - CO - S_2$ is very efficient for $\mathbf{4}$ (35% in the mass spectrum) and the OCCCSS connectivity has been recently assigned to the $m/z$ 116 ions [13].
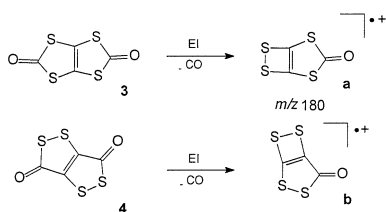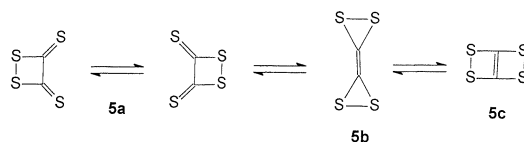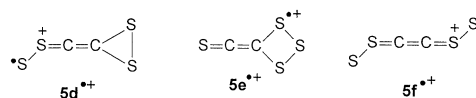


Scheme 3.

### 3.2. Collision-induced dissociations and neutralization–reionization experiments of $C_2S_4^{\cdot+}$ (m/z 152) radical cations

Surprisingly, the CA spectra of the $C_2S_4^{\cdot+}$ ($m/z$ 152) radical cations, prepared starting from the isomeric $\mathbf{3}$ and $\mathbf{4}$ precursors, are found to be identical [Fig. 1(a)]. The so-produced ions have therefore the same structure or different structures separated by a low-energy isomerization barrier allowing facile interconversion. The signal at $m/z$ 88 (loss of $S_2$) constitutes the base peak of these spectra and corresponds to the molecular ions of ethene dithione, $SCCS^{\cdot+}$. The collision-excited ions also expel intensively neutral carbon disulfide ($m/z$ 76, formation of $CS_2^{\cdot+}$ ions). It is worthwhile to note that this reaction is already occurring without the presence of the collision gas and could possibly be associated with a rearrangement reaction. The formation of ethene dithione ions could be in keeping with the formation of a cyclic species like the molecular ion of 1,2-dithiane-3,4-dithione ($\mathbf{5a}^{\cdot+}$). The neutral counterpart of this ion and some of its valence isomers have been studied theoretically [14]. Amongst some possible valence structures shown in Scheme 3, structure $\mathbf{5a}$ was calculated to be the global minimum on the potential energy surface. However, to the best of our knowledge, this neutral molecule has not yet been observed experimentally.

If valence isomerism also occurs in the $\mathbf{5a}^{\cdot+}$ radical cations, other $C_2S_4^{\cdot+}$ candidates should be considered and some of these structures are depicted in Scheme 4.

Neutralization–reionization mass spectrometry



Scheme 2.



Scheme 4.

(NRMS) has been recognized as a valuable tool for the production and characterization of neutral reactive molecules in the gas phase and fast identification of noncovalently bounded species (protonated dimers, ion–molecule complexes, etc.) [15]. Given the deposition of a higher internal energy in the ions during the reionization step, NRMS also affords in some instances more structural information than CA (unimolecular reactions of metastable ions are usually of very low abundance in NR).

Sequential reduction of the $m/z$ 152 ions by collision with xenon and reionization with oxygen gives the NR spectrum presented in Fig. 1(b). Although featuring only a very low intensity recovery signal for survivor ions, its observation reveals that the neutral species could be a stable molecule in the gas phase, at least during the time of flight between the two collision cells (a fraction of a microsecond). The fragmentations observed in the NR spectrum are moreover in keeping with those observed in the corresponding CA experiment [Fig. 1(a)]. The large intensity increase of the $m/z$ 64 ($S_2^{\cdot+}$ ions) peak is due to the ionization of neutrals generated in the neutralization cell by unimolecular or/and collision-induced dissociations (formation of $m/z$ 88 ions in the CA experiment). The observation of such an increase is important as it confirms that the production of SCCS$^{\cdot+}$ ions in the CA experiment [$m/z$ 88, Fig. 1(a)] results from the loss of $S_2$ rather than two sulfur atoms, this observation represents a good experimental evidence for the formation of a covalently bounded species like $\mathbf{5a}$–$\mathbf{f}^{\cdot+}$ radical cations.

The CA spectrum of the $C_2S_4^{\cdot+}$ ions produced by chemical ionization [Fig. 1(c)] is quite different and dominated by the signal at $m/z$ 76 ($CS_2^{\cdot+}$ radical cations). Moreover, the peak at $m/z$ 88 is of very low intensity. The NR spectrum [Fig. 1(d)] does not feature any recovery signal and is also dominated by the signal corresponding to carbon disulfide molecular ions ($m/z$ 76). The comparison of the different spectra [Fig. 1(a) and (c); Fig. 1(b) and (d)] clearly reveals that the ions obtained in the chemical ionization ion source differ from the ions obtained by dissociative ionization of **3** (and **4**). The observed differences can be readily explained on the basis of the formation of

a covalently bounded ion in the case of the dissociative ionization and of an ion–molecule complex between carbon disulfide molecular ion and neutral carbon disulfide for the ions produced in the CI source.
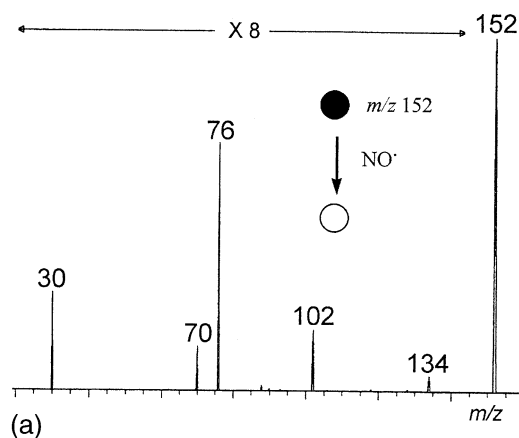
### 3.3. Low energy collision-induced dissociations of $C_2S_4^{\cdot+}$ (m/z 152) radical cations

In its hybrid configuration, the AutoSpec 6F mass spectrometer also allows the study of collision-induced dissociations in the low kinetic energy regime, typically 20–30 eV. When $C_2S_4^{\cdot+}$ ions produced from **3** or **4** are submitted to collision with argon in the quadrupolar collision cell, two signals corresponding to the losses of neutral $CS_2$ ($m/z$ 76) and $S_2$ ($m/z$ 88) are recorded. In contrast, the $C_2S_4^{\cdot+}$ ions generated under chemical ionization conditions eliminate only $CS_2$ ($m/z$ 76) after collisional activation. These observations compare thus perfectly with the high energy collisional activation experiments. Particularly, the loss of $S_2$ ($m/z$ 88) is indicative of the presence of such a group in the covalently bounded species.

### 3.4. Ion–molecule reactions with nitric oxide

Fig. 2(a) shows the result of ion–molecule reactions of mass-selected $C_2S_4^{\cdot+}$ ions with nitric oxide in the rf-only quadrupole collision cell. Beside the unimolecular fragmentation ($m/z$ 76) and charge exchange (NO$^+$, $m/z$ 30), the ion–molecule reaction products are clearly indicated by peaks at $m/z$ 134 ($C_2S_4^{\cdot+}$ + NO$^{\cdot}$ − SO), $m/z$ 102 ($C_2S_4^{\cdot+}$ + NO$^{\cdot}$ − OS$_2$) and $m/z$ 70 ($C_2NS^+$ ions). The formation of these ions can be accommodated starting with a complex between $C_2S_4^{\cdot+}$ ion and nitric oxide (Scheme 5) which dissociate by losing SO or the disulfur analogue of ozone, OS$_2$. The $m/z$ 70 signal being the base peak of the CA spectrum of the $m/z$ 102 ions [Fig. 2(b)], it can be concluded that $m/z$ 102 ion partly loses a sulfur atom yielding $C_2NS^+$ ion ($m/z$ 70).

The behaviour of the $C_2S_4^{\cdot+}$ ions formed by chemical ionization is completely different, the main reaction being the displacement of $CS_2$ by NO$^{\cdot}$ with the formation of an ion–molecule complex [$CS_2$/NO]$^+$ ($m/z$ 106).

(a)



Scheme 5.

mass-selected $m/z$ 129 ions shown in Fig. 3(b) features an intense peak at $m/z$ 88 which may correspond to ionized ethene dithione suggesting that these ions consist of a complex between $C_2S_2$ and $CH_3NC$ (Scheme 6).
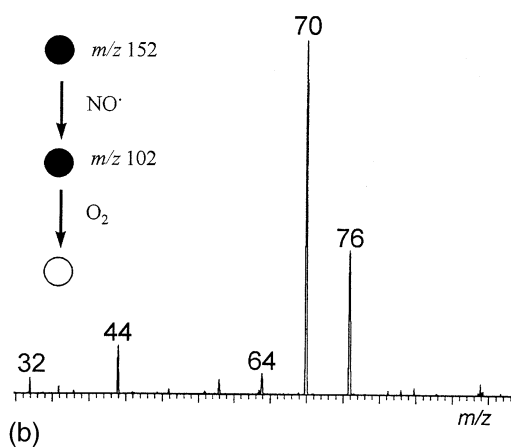


(b)

Fig. 2. Ion–molecule reactions of the $C_2S_4^{\cdot+}$ ions ($m/z$ 152), generated by dissociative ionization of **3**, with nitric oxide: (a) mass spectrum of the ion–molecule products and (b) CA ($O_2$, linked scan) of the $m/z$ 102 cations.

### 3.5. Ion–molecule reactions with methyl isocyanide, CH₃NC

Methyl isocyanide appears also very reactive towards the $m/z$ 152 ions generated from **3**. The main products are observed at $m/z$ 129 and 120 [Fig. 3(a)] and corresponds, respectively, to the displacement of $S_2$ by $CH_3NC$ and to the transfer of sulfur to methyl isocyanide with charge retention on $C_2S_3$. The CA spectrum of
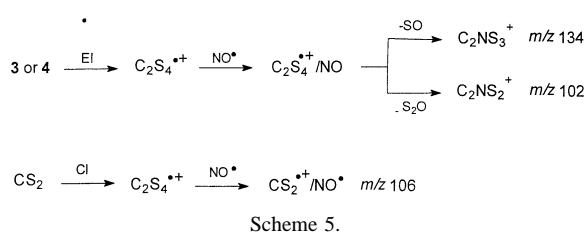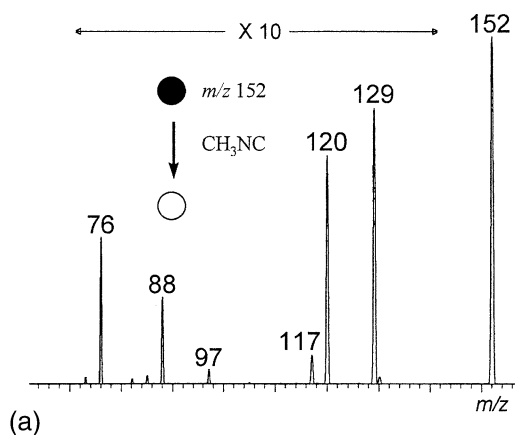


(a)



(b)

Fig. 3. Ion–molecule reactions of the $C_2S_4^{\cdot+}$ ions, generated by dissociative ionization of **3**, with methyl isocyanide: (a) mass spectrum of the ion–molecule products and (b) CA ($O_2$, linked scan) of the $m/z$ 129 cations.
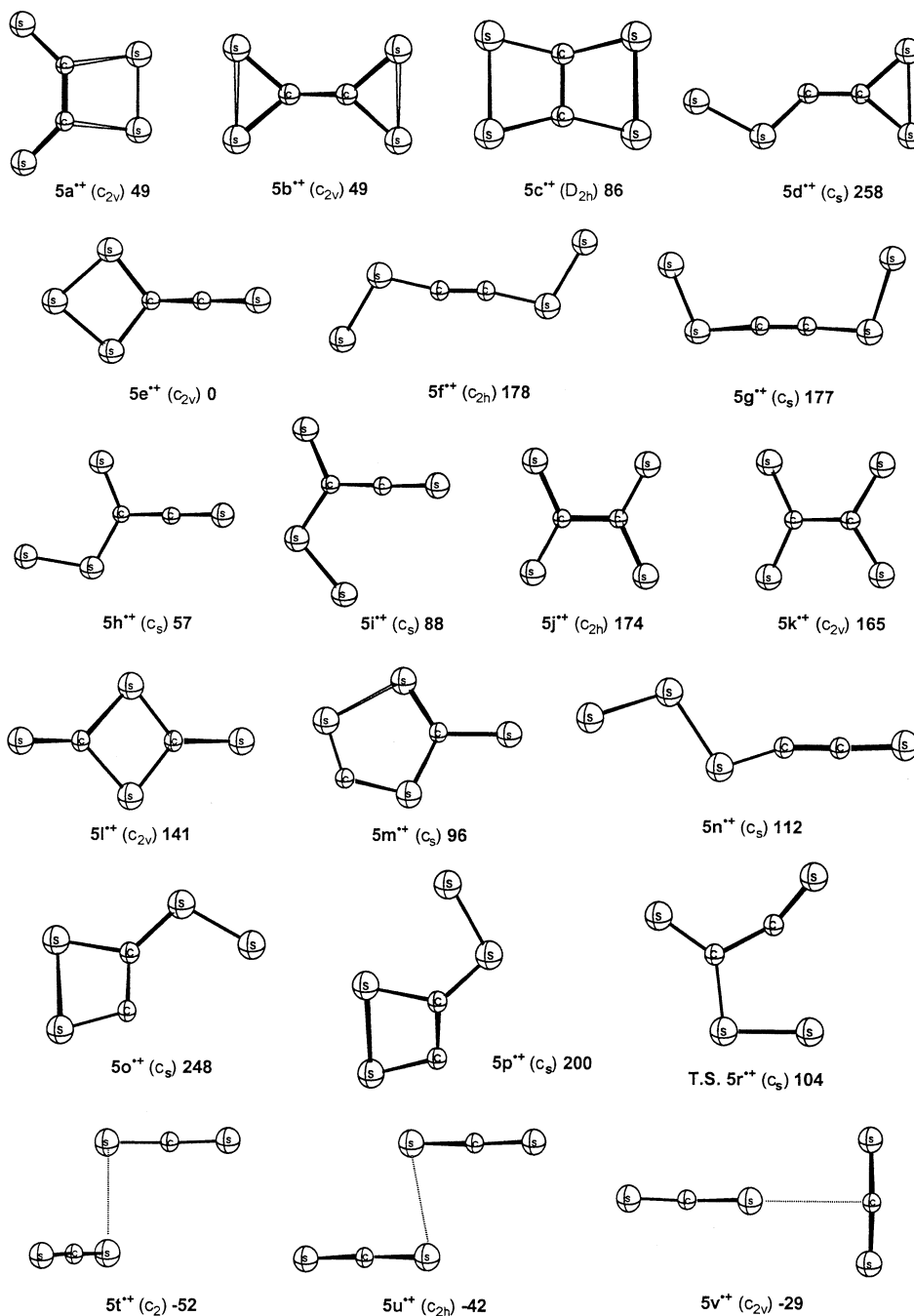
$$CH_3NC$$

$$C_2S_3^{\bullet+} \longleftarrow C_2S_4^{\bullet+} \xrightarrow{CH_3NC} CH_3NC/C_2S_2^{\bullet+}$$

$$m/z\ 120 \qquad\qquad\qquad\qquad\qquad m/z\ 129$$

$$\downarrow CH_3NCS \qquad\qquad \downarrow S_2$$

$$CS_2 \xrightarrow{Cl} C_2S_4^{\bullet+} \xrightarrow{CH_3NC} CS_2^{\bullet+}/CH_3NC$$

$$\downarrow CS_2 \qquad\qquad m/z\ 117$$

Scheme 6.

The chemistry of the cluster $C_2S_4^{\cdot+}$ ion is completely different and consists of the net displacement of neutral $CS_2$ by methyl isocyanide with the formation of a new ionized complex $CH_3CN/CS_2^{\cdot+}$ detected at $m/z$ 117.

Even at quasithermal kinetic energies, we have not been able to detect any signals for the $C_2S_4/NO$ and $C_2S_4/CH_3NC$ complexes, probably due to the absence of ion thermalization in our experiments. We therefore turned to high level molecular orbital calculations in order to estimate relative energies of the most plausible $C_2S_4^{\cdot+}$ isomeric radical cations.

## 4. Molecular orbital calculations

### 4.1. Computational methods

Standard ab initio calculations are carried out with the GAUSSIAN 98 series of programs [16]. The structures and energies of $C_2S_4^{\cdot+}$ radical cations, related fragments, and ion–molecule reaction products are examined at the G2(MP2,SVP) level of theory [17]. This corresponds effectively to QCISD(T)/6-311+G(3df,2p)//MP2/6-31G* energies together with zero-point vibrational and isogyric corrections. Spin-restricted calculations are used for closed-shell systems, and spin-unrestricted ones for open-shell systems.

### 4.2. $C_2S_4^{\cdot+}$ isomeric structures

We have investigated here for the first time the various covalently bounded $C_2S_4^{\cdot+}$ structures. Sixteen isomeric structures ($5a^{\cdot+}$–$5p^{\cdot+}$, Fig. 4) are considered and are all predicted to be stable equilibrium structures, characterized by all real vibrational frequencies (HF/6-31G*). The most stable structure is the four-membered ring thioketene structure ($5e^{\cdot+}$). 1,2-dithietane-3,4-dithione ($5a^{\cdot+}$) and bidithiiranyl ($5b^{\cdot+}$) radical cations lie close in energy, both species are 49 kJ mol$^{-1}$ above $5e^{\cdot+}$. The open-chained thioketene isomers ($5h^{\cdot+}$ and $5i^{\cdot+}$) are slightly higher in energy than the cyclic isomer $5e^{\cdot+}$. Other $S$-sulfides structures ($5d^{\cdot+}$, $5f^{\cdot+}$, $5g^{\cdot+}$, $5n^{\cdot+}$, $5o^{\cdot+}$, and $5p^{\cdot+}$) are predicted to be significantly higher in energy. Interestingly, both opened $CS_2CS_2^{\cdot+}$ structures ($5j^{\cdot+}$ and $5k^{\cdot+}$) are not energetically favorable. It seems that formation of a cyclic structure is generally favorable in this sulfur-containing system.

There are some interesting structural features of the $C_2S_4^{\cdot+}$ ions that warrant discussion. Most of the cyclic compounds considered here are characterized by a rather long C–S or S–S bond in the ring. For instance, the C–S bond length in $5a^{\cdot+}$ is 1.982 Å, which suggests that C–S bond cleavage in $5a^{\cdot+}$ is rather easy. Indeed, ring opening of $5a^{\cdot+}$ to $5i^{\cdot+}$ by way of transition state $5r^{\cdot+}$, is calculated to have a small barrier of 55 kJ mol$^{-1}$. Likewise, both bicyclic isomers $5b^{\cdot+}$ and $5c^{\cdot+}$ have long S–S bond lengths,

Fig. 4. Structures and relative energies (kJ mol$^{-1}$, G2(MP2,SVP) of isomeric $C_2S_4^{\cdot+}$ radical cations.

2.246 and 2.221 Å, respectively. For comparison, the S–S single bond length in $H_2S_2$ is 2.071 Å (MP2/6-31G*). The $CS_2 \cdot \cdot CS_2^{\cdot+}$ molecular ions have been examined recently by Zhou and Andrews [18]. In agreement with the DFT calculations by Zhou and Andrews, the $C_2$-like structure is the most stable
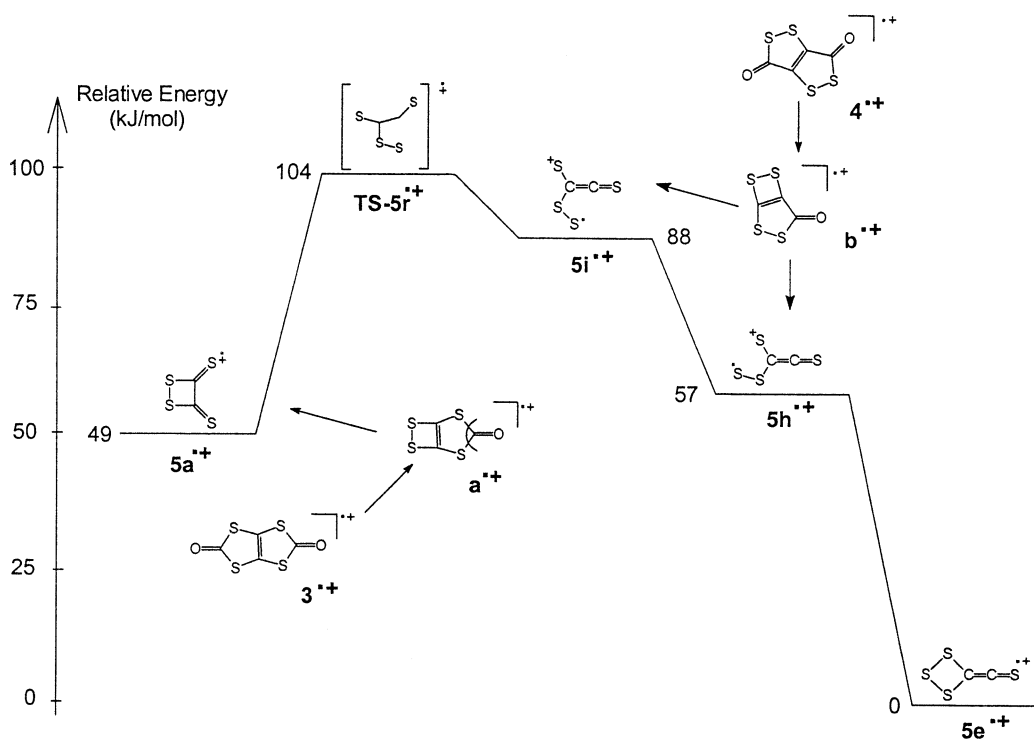
Fig. 5. Potential energy profile for some isomerization processes connecting $C_2S_4^{.+}$ radical cations.

structure of the three dimer ions ($5t^{.+}$, $5u^{.+}$, and $5v^{.+}$, Fig. 4). However, the $C_2$ structure is predicted to have a distorted form at the MP2/6-31G* level. The planar $C_{2h}$ ($5u^{.+}$) and the T-shape $C_{2v}$ ($5v^{.+}$) structures are 10 and 23 kJ mol$^{-1}$, respectively, less stable than $5t^{.+}$. The calculated S. . .S distance in the dimer ion complex $5t^{.+}$ is 2.852 Å and the binding energy, with respect to $CS_2 + CS_2^{.+}$, is reasonably large (77 kJ mol$^{-1}$). This van der Waals complex is more stable than the most stable covalently bounded $C_2S_4^{.+}$ ion ($5e^{.+}$) by 52 kJ mol$^{-1}$.

Based on the molecular structures of the precursor molecule 3, it is conceivable that the dissociative ionisation of 3, by way of the intermediate ion a, initially leads to the cyclic radical cation $5a^{.+}$ (Fig. 5). This radical cation can easily undergo a ring opening (cleavage of a single C–S bond, vide supra) to yield the distonic radical cation $5i^{.+}$ by way of TS- $5r^{.+}$. At this step, the radical cation $5i^{.+}$ may reasonably be

expected to collapse to the most stable covalently bonded ion $5e^{.+}$, by way of the open-chained thioketene isomer ($5h^{.+}$)

Since rearrangement of $5a^{.+}$ is predicted to have a small activation barrier [TS ($5a^{.+} \rightarrow 5i^{.+}$) = 55 kJ/mol], it is likely that $5a^{.+}$, $5h^{.+}$, and $5e^{.+}$ coexist in the high energy condition of the mass spectrometry experiments and that the observed CA spectra arise from the fragmentation reactions of these isomers.

Thus, we have calculated the unimolecular fragmentation and rearrangement reactions of both $5a^{.+}$ and $5h^{.+}$ using the G2(MP2,SVP) theory (Table 1). For the open-chained isomer $5h^{.+}$, dissociation to $S_2 + C_2S_2^{.+}$ ($m/z$ 88) represents the lowest-energy fragmentation process. Loss of $C_2S_2$ and CS are the next most favorable dissociation reactions. The simple C–S and S–S bond cleavage processes, leading to the formation of $C_2S_3^{.+}$ ion (SCCSS$^{.+}$ or SCCS$_2^{.+}$) are significantly higher in energy. For the cyclic isomer

Table 1
Calculated fragmentation energies[a] of $C_2S_4^{*+}$ ions (**5a**$^{\cdot+}$ and **5h**$^{\cdot+}$)

| Species | Relative energy | Species | Relative energy |
|---|---|---|---|
| SC(S)C(S)S$^{\cdot+}$ (**5a**$^{\cdot+}$) | 0.0 | SCC(S)SS$^{\cdot+}$ (**5h**$^{\cdot+}$) | 0.0 |
| Ring opening T.S. (**5r**$^{\cdot+}$) | 55.3 | S$_2$ + SCCS$^{\cdot+}$ (*m/z* 88) | 130.9 |
| CS$_2$ + CS$_2^{\cdot+}$ (*m/z* 76) | −24.4 | SCCS + S$_2^{\cdot+}$ (*m/z* 64) | 196.8 |
| S$_2$ + SCCS$^{\cdot+}$ (*m/z* 88) | 169.6 | CS + CS$_3^{\cdot+}$ (*m/z* 108) | 250.7 |
| SCCS + S$_2^{\cdot+}$ (*m/z* 64) | 235.6 | S + SCCS$_2^{\cdot+}$ (*m/z* 120) | 367.8 |
| S + SSCCS$^{\cdot+}$ (*m/z* 120) | 445.5 | S + SCCSS$^{\cdot+}$ (*m/z* 120) | 459.0 |
| SSCCS + S$^{\cdot+}$ (*m/z* 32) | 757.6 | CS$_3$ + CS$^{\cdot+}$ (*m/z* 44) | 487.7 |
| | | SCCS$_2$ + S$^{\cdot+}$ (*m/z* 32) | 603.8 |
| | | SCCSS + S$^{\cdot+}$ (*m/z* 32) | 629.3 |

[a] G2(MP2, SVP) level. G2(MP2, SVP) $E_0$ energies include −1666.668 13 (**5a**$^{\cdot+}$), and −1666.653 38 (**5h**$^{\cdot+}$) Hartrees.

**5a**$^{\cdot+}$, dissociation to $CS_2$ + $CS_2^{\cdot+}$ (*m/z* 76) is calculated to be an exothermic process ($-24$ kJ mol$^{-1}$). Loss of S$_2$ is also energetically favorable.

As far as the dissociative ionization of precursor **4** is concerned, the loss of CO from the intermediate radical cation **b**, see Scheme 2 and Fig. 5, could initially lead to the radical cation **5h**$^{\cdot+}$ and/or **5i**$^{\cdot+}$. The calculated facile isomerization between **5a**$^{\cdot+}$ and **5h**$^{\cdot+}$ is in excellent accord with the experimental observation that identical CAMS is observed from both the different precursors of $C_2S_4^{\cdot+}$ ion. Indeed, the predicted dominant fragments, $CS_2^{\cdot+}$ (*m/z* 76) and $C_2S_2^{\cdot+}$ (*m/z* 88) from **5a**$^{\cdot+}$ and **5h**$^{\cdot+}$, respectively, are readily seen as dominant peaks in the observed CAMS [Fig. 1(a)].

The existence of both **5a**$^{\cdot+}$ and **5h**$^{\cdot+}$ radical cations in the ion beam is also consistent with the observed ion–molecule reactions in the case of methyl isocyanide neutral reagent. Actually, as shown in Scheme 6, $C_2S_4^{\cdot+}$ radical ions react with the neutral reagent (1) by $S_2$/CH$_3$NC substitution in the ion and (2) by sulfur transfer to the neutral reagent. The former reaction could be attributed to the presence of **5a**$^{\cdot+}$ ions

whereas **5h**$^{\cdot+}$, having an *S*-sulfide connectivity, could be responsible to the latter reaction. Indeed, carbon disulfide *S*-sulfide radical cations, SCSS$^{\cdot+}$, for instance, was demonstrated to efficiently transfer S$^{\cdot+}$ to several nitriles [3], isocyanides [19], azines [20], and thioethers [21].

### 4.3. Ion–molecule reaction with NO·

We have examined the ion–molecule reaction of the $C_2S_4^{\cdot+}$ ions (**5**$^{\cdot+}$) with nitric oxide (NO·). Since the four-membered ions **5a**$^{\cdot+}$ and **5e**$^{\cdot+}$ are likely to be less reactive, only the open-chained isomer **5h**$^{\cdot+}$ is considered here. Experimentally, the ion–molecule reactions lead to two major fragment products (losses of SO and S$_2$O from the collision complex). Formation of SO or SO$_2$ requires cleavage of the N−O bond in the [$C_2S_4^{\cdot+}$−NO·] ion complex. This suggests that the structure of ion complex is likely to be a cyclic species. We have investigated several plausible singlet (S) and triplet (T) structures of [$C_2S_4^{\cdot+}$−NO·] complex, and their optimized geometries and calculated enthalpies of formation are summarized in Fig. 6. Amongst all the species considered here, the five-membered triplet ion **T6c** is the most stable structure. The calculated enthalpy of formation, with respect to $C_2S_4^{\cdot+}$ (**5h**$^{\cdot+}$) + NO·, is $-5$ kJ mol$^{-1}$. Dissociation of **T6c** to SO + S$_2$CC(S)N$^+$ (*m/z* 134) is predicted to be a slightly endothermic process (49 kJ mol$^{-1}$). Ion complexes **S6a** and **T6b** are the likely species which fragment to give S$_2$O. Loss of S$_2$O is calculated to be an energetically favorable process for both **S6a** and **T6b**. In summary, the calculated results support the experimental findings for ion–molecule reaction between $C_2S_4^{\cdot+}$ and NO·.

## 5. Conclusions

A combination of tandem mass spectrometric techniques (collisional activation, neutralization-reionization, ion-molecule reactions) and high level molecular orbital calculations has allowed the identification of several isomeric $C_2S_4^{\cdot+}$ radical cations:
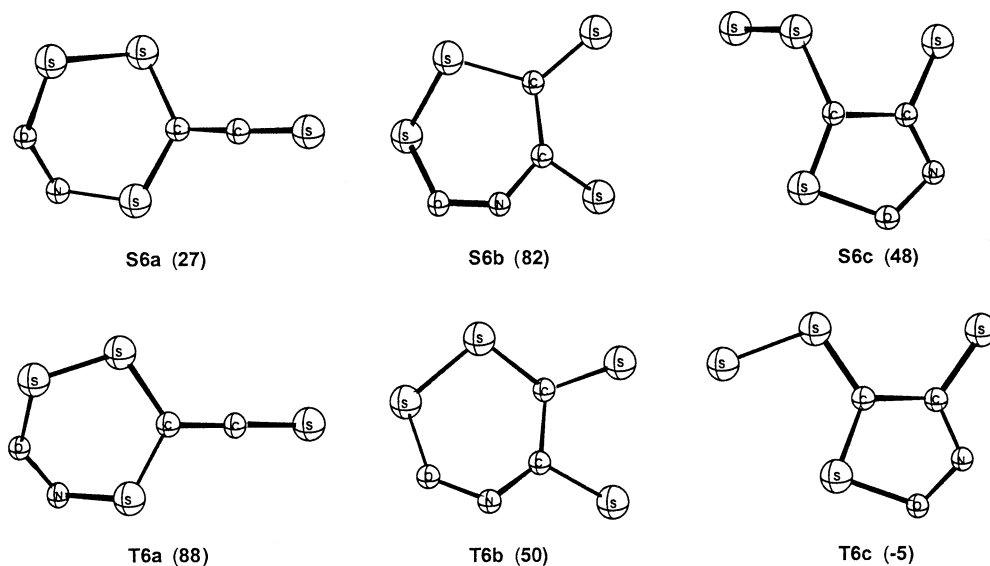
Fig. 6. Structures and enthalpies of formation (kJ mol$^{-1}$) of [$C_2S_4^{\cdot+}\cdots$NO$^{\cdot}$] complexes.

a dimer $CS_2/CS_2^{\cdot+}$ generated during carbon disulfide chemical ionization and some easily interconverting covalently bounded species generated by dissociative ionization of isomeric dithiolodithioles. As far as the covalently bounded radical cations are concerned, the experimental and theoretical results are interpreted by the coexistence, whatever the precursor is, of easily interconverting **5a**$^{\cdot+}$, **5h**$^{\cdot+}$, and **5e**$^{\cdot+}$ radical cations. The ion–molecule complex is calculated 52 kJ mol$^{-1}$ more stable than the covalently bounded species.

## References

[1] M.-T. Praet, J.P. Delwiche, Adv. Mass Spectrom. 6 (1974) 829.
[2] (a) C. Wentrup, P. Kambouris, R.A. Evans, D. Owen, G. Macfarlane, J. Chuche, J.C. Pommelet, A. Ben Cheikh, M. Plisnier, R. Flammang, J. Am. Chem. Soc. 113 (1991) 3130; (b) D. Sülzle, H. Schwarz, Angew. Chem. Int. Ed. Engl. 27 (1988) 1337: (c) M. Plisnier, Ph.D. thesis, University of Mons-Hainaut, 1992; (d) G. Maier, H.P. Reisenauer, R. Ruppel, Sulfur Rep. 21 (1999) 335; (e) R. Flammang, C. Wentrup, ibid. 21 (1999) 357; (f) R.R. Bohn, Y. Hannachi and L. Andrews, J. Am. Chem. Soc. 114 (1992) 6452.
[3] P. Gerbaux, Y. Van Haverbeke, R. Flammang, M.W. Wong, C. Wentrup, J. Phys. Chem. A 101 (1997) 6970.
[4] D. Sülzle, H. Egsgaard, L. Carlsen, H. Schwarz, J. Am. Chem. Soc. 112 (1990) 3750.
[5] P. Gerbaux, R. Flammang, C.Th. Pedersen, M.W. Wong, J. Phys. Chem. A 103 (1999) 3666.
[6] P. Gerbaux, Ph.D. Thesis, University of Mons-Hainaut, 1999.
[7] M.W. Wong, C. Wentrup, R. Flammang, J. Phys. Chem. 99 (1995) 16849.
[8] ixR.H. Bateman, J. Brown, M. Lefevere, R. Flammang, Y. Van Haverbeke, Int. J. Mass Spectrom. Ion Processes 115 (1992) 205.
[9] R. Flammang, Y. Van Haverbeke, C. Braybrook, J. Brown, Rapid Commun. Mass Spectrom. 9 (1995) 795.
[10] A.M. Richter, E. Fanghänel, Tetrahedron Lett. 24 (1983) 3577.
[11] (a) M.E. Gress, S.H. Linn, Y. Ono, H.F. Prest, C.Y. Ng, J. Chem. Phys. 72 (1980) 4242; (b) Y. Ono, S.H. Linn, H.F. Prest, M.E. Gress, C.Y. Ng, ibid. 74 (1981) 1125.

[12] A. Pelc, L. Michelak, Int. J. Mass Spectrom. 194 (2000) 85.

[13] C.Th. Pedersen, R. Flammang, P. Gerbaux, E. Fanghänel, J. Chem. Soc., Perkin Trans. 2 (1998) 1403.

[14] G. Calzaferri, R. Gleiter, J. Chem. Soc., Perkin Trans. 2 (1975) 559.

[15] C.A. Schalley, G. Hornung, D. Schröder, H. Schwarz, Chem. Soc. Rev. 27 (1998) 91.

[16] M.J. Frisch, G.W. Trucks, H.B. Schlegel, G.E. Scuseria, M.A. Robb, J.R. Cheeseman, V.G. Zakrzewski, J.A. Montgomery Jr., R.E. Stratmann, J.C. Burant, S. Dapprich, J.M. Millam, A.D. Daniels, K.N. Kudin, M.C. Strain, O. Farkas, J. Tomasi, V. Barone, M. Cossi, R. Cammi, B. Mennucci, C. Pomelli, C. Adamo, S. Clifford, J. Ochterski, G.A. Petersson, P.Y. Ayala, Q. Cui, K. Morokuma, D.K. Malick, A.D. Rabuck, K. Raghavachari, J.B. Foresman, J. Cioslowski, J.V. Ortiz, A.G. Baboul, B.B. Stefanov, G. Liu, A. Liashenko, P. Piskorz, I. Komaromi, R. Gomperts, R.L. Martin, D.J. Fox, T. Keith, M.A. Al-Laham, C.Y. Peng, A. Nanayakkara, C. Gonzalez, M. Challacombe, P.M.W. Gill, B. Johnson, W. Chen, M.W. Wong, J.L. Andres, C. Gonzalez, M. Head-Gordon, E.S. Replogle, J.A. Pople, GAUSSIAN 98, Gaussian Inc., Pittsburgh, PA, 1998.

[17] L.A. Curtiss, P.C. Redfern, B.J. Smith, L. Radom, J. Chem. Phys. 104 (1996) 5148.

[18] M. Zhou, L.J. Andrews, Chem. Phys. 112 (2000) 15.

[19] P.Gerbaux, Ph.D. thesis, University of Mons-Hainaut, 1999.

[20] P. Gerbaux, Y. Van Haverbeke, R. Flammang, J. Mass Spectrom. 32 (1997) 1170.

[21] P. Gerbaux, J.-Y. Salpin, G. Bouchoux, R. Flammang, Int. J. Mass Spectrom., 195/196 (2000) 239.

[22] J.C. Schwartz, A.P. Wade, C.G. Enke, R.G. Cooks, Anal. Chem. 62 (1990) 1809.